Accepted Manuscript

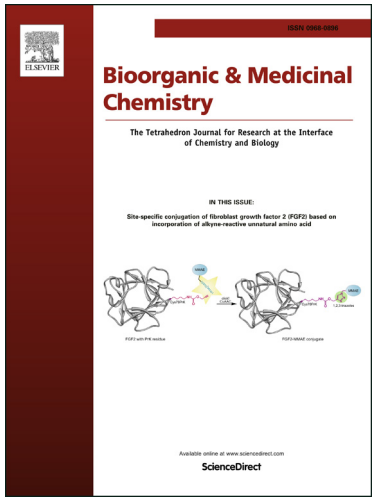

Discovery of new leads against *Mycobacterium tuberculosis* using Scaffold Hopping and Shape based Similarity

Ravindra D. Wavhale, Elvis A.F. Martis, Premlata K. Ambre, Baojie Wan, Scott G Franzblau, Krishna R. Iyer, Kavita Raikuvar, Katarzyna Macegoniuk, Łukasz Berlicki, Santosh R. Nandan, Evans C. Coutinho

PII: S0968-0896(17)30612-0
DOI: http://dx.doi.org/10.1016/j.bmc.2017.07.034
Reference: BMC 13871

To appear in: *Bioorganic & Medicinal Chemistry*

Received Date: 27 March 2017
Revised Date: 30 June 2017
Accepted Date: 17 July 2017

Please cite this article as: Wavhale, R.D., Martis, E.A.F., Ambre, P.K., Wan, B., Franzblau, S.G., Iyer, K.R., Raikuvar, K., Macegoniuk, K., Berlicki, L., Nandan, S.R., Coutinho, E.C., Discovery of new leads against *Mycobacterium tuberculosis* using Scaffold Hopping and Shape based Similarity, *Bioorganic & Medicinal Chemistry* (2017), doi: http://dx.doi.org/10.1016/j.bmc.2017.07.034

Discovery of new leads against *Mycobacterium tuberculosis* using Scaffold Hopping and Shape based Similarity

Ravindra D. Wavhale[±], Elvis A. F. Martis[±], Premlata K. Ambre[±], Baojie Wan[§], Scott G Franzblau[§], Krishna R. Iyer[±], Kavita Raikuvar[±], Katarzyna Macegoniuk[ˀ], Łukasz Berlicki[ˀ], Santosh R. Nandan[⊥] and Evans C. Coutinho[±†]

[±]Department of Pharmaceutical Chemistry, Bombay College of Pharmacy, Kalina, Mumbai 400098, India.

[⊥]Ambernath Organics, 307/314, Creative Industries Premises, Kalina, Mumbai 400098, India.

[§]Institute for Tuberculosis Research, University of Illinois, Chicago 60612, USA.

[ˀ]Department of Bioorganic Chemistry, Wroclaw University of Technology, Wroclaw 50-370, Poland.

[†]**For Correspondence**: E-mail: evans.coutinho@bcp.edu.in
Tel No. +91-22-26670905. Fax No. +91-22-26670816

Graphical Abstract

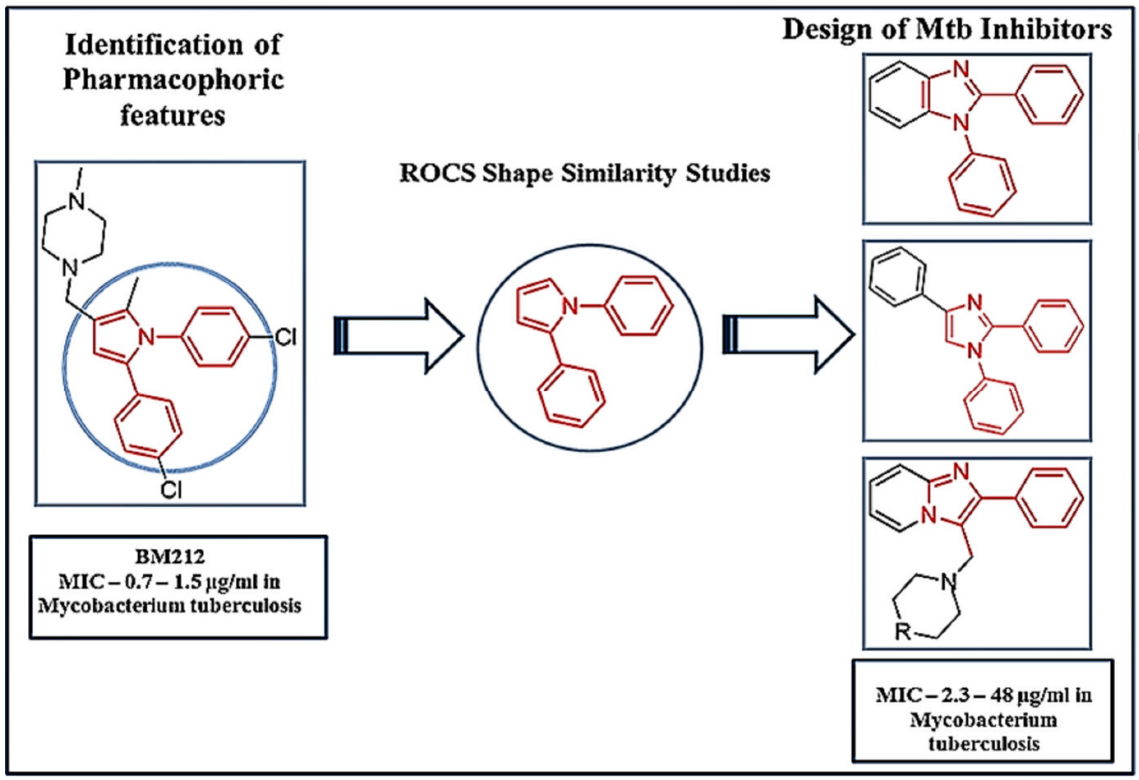

Abstract

BM212 [1,5-diaryl-2-methyl-3-(4-methylpiperazin-1-yl)-methyl-pyrrole] is a pyrrole derivative with strong inhibitory activity against drug resistant *Mycobacterium tuberculosis* and mycobacteria residing in macrophages. However, it was not pursued because of its poor pharmacokinetics and toxicity profile. Our goal was to design and synthesize new antimycobacterial BM212 analogues with lower toxicity and better pharmacokinetic profile. Using the scaffold hopping approach, three structurally diverse heterocycles - 2,3-disubstituted imidazopyridines, 2,3-disubstituted benzimidazoles and 1,2,4-trisubstituted imidazoles emerged as promising antitubercular agents. All compounds were synthesized through easy and convenient methods and their structures confirmed by IR, ^{1}H NMR, ^{13}C NMR and MS. In-vitro cytotoxicity studies on normal kidney monkey cell lines and HepG2 cell lines, as well as metabolic stability studies on rat liver microsomes for some of the most active compounds, established that these compounds have negligible cytotoxicity and are metabolically stable. Interestingly the benzimidazole compound **(4a)** is as potent as the parent molecule BM212 (MIC 2.3 µg/ml vs 0.7-1.5 µg/ml), but is devoid of the toxicity against HepG2 cell lines (IC_{50} 203.10 µM vs 7.8 µM).

Key-words: BM212, scaffold hopping, anti-tubercular activity, microplate alamar blue assay, 2,3-disubstituted benzimidazoles, 1,2,4-trisubstituted imidazoles, 2,3-disubstituted imidazopyridines, *Mycobacterium tuberculosis.*

	Cytotoxicity	Metabolic stability
M. tuberculosis		

1 Introduction

The WHO report 2016 gives an estimate of 10.4 million new TB cases with 1.4 million TB deaths in 2015[1]. In recent times, drug resistance has emerged as the greatest problem. As a result, physicians are left with limited choice of drugs, increasing the risk of therapy failures. Deidda *et al*. had identified BM212, a 1,5-diarylpyrrole derivative, with promising activity against multidrug-resistant clinical isolates of *Mycobacterium tuberculosis* and also against those residing within macrophages (MICs between 0.7 and 1.5 μg/ml)[2]. These results offered a ray of hope for the emergence of a new anti-tubercular agent (**Figure 1**), however it was soon realized that BM212 suffers from poor bioavailability and severe toxicity. In the pursuit of new derivatives of BM212 with improved pharmacokinetics and toxicity profile[3-7], optimization strategies were focused on modification of the 1,5-diphenyl substituents and the side chain at the 3-position of the pyrrole ring. Several **BM212** analogues like BM521, BM533, BM579 and Compound I were synthesized with good biological profiles (MIC ranging from 0.2 to 0.12 μM) and comparatively better Protection Indices (PI = CC_{50}/MIC, ranging from 127.5 to 1937.5) than BM212 (**Figure 1**), but all suffer from high HepG2 toxicity[6] (**Table 1**).

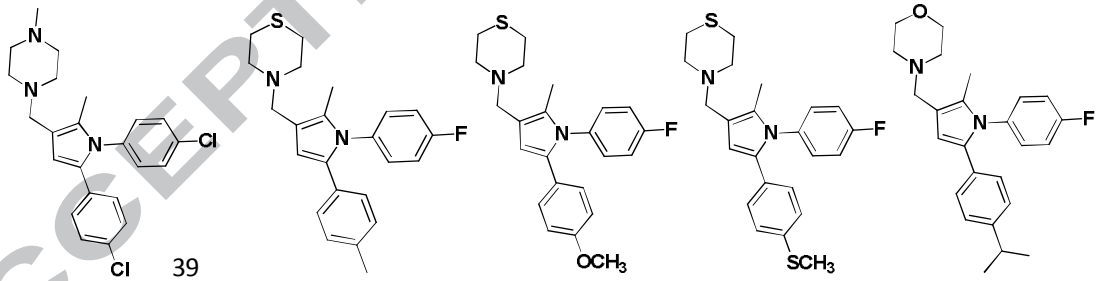

BM212 BM521 BM533 BM579 I

Figure 1 BM212 and their analogs

		VERO cells	HepG2Cells	clearance in mouse microsomes
		IC_{50} (μM)	IC_{50} (μM)	$T_{1/2}$ (Min)
BM212	5	-	7.8	>30
BM521	0.16	178.80	24.01	8.2
BM533	0.20	>302.26	>2423.77	<5
BM579	0.16	15.20	5.90	10
I	0.12	50.15	15.3	>30

Table 1 In vitro cytotoxicity on VERO cells and HEPG2 cells and metabolic stability studies of BM212 and analogs[6].

To further augment the safety and efficacy profile of BM212 and develop potent antitubercular agents through exploration of the diversity in the chemical space of BM212, we embarked on the scaffold hopping approach to seek a replacement for the central pyrrole ring in BM212. This strategy identified imidazole, benzimidazole and imidazopyridine scaffolds as promising replacement moieties. Furthermore, the Rapid Overlay of Chemical Structures[8-10] (ROCS) program was employed to search analogs of these three scaffolds with similar 3D shape and volume outlines as BM212. The Tanimoto shape similarity coefficient (TSSC) was used to quantify the shape similarity, and those molecules with TSSC greater than 0.60 were advanced for further studies. This approach led to a library of twenty compounds comprising 1,2,4-trisubstituted imidazoles, 2,3-disubstitued benzimidazoles and 2,3-disubstituted imidazopyridines. These compounds were profiled for their antimycobacterial activity and cytotoxicity potential.

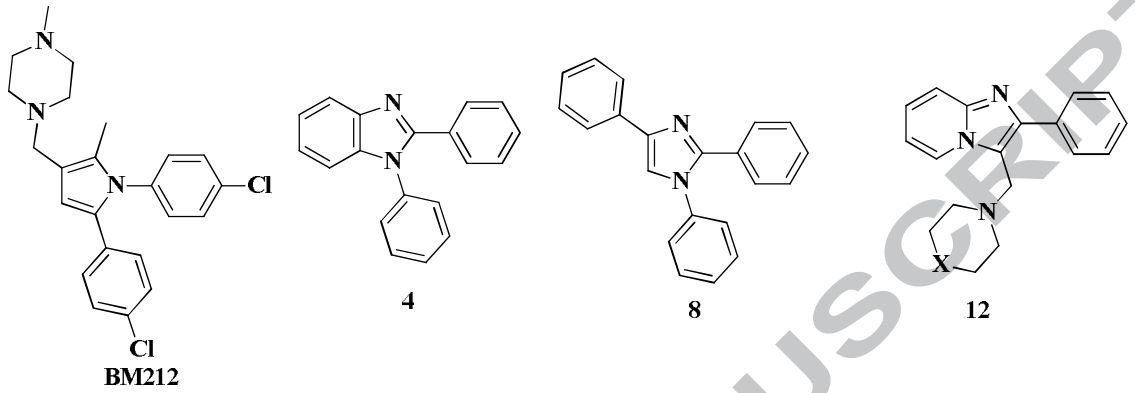

Figure 2: BM212 and representative molecules belonging to the scaffolds benzimidazole (**4**), imidazole (**8**), and imidazopyridine (**12**) that were designed using scaffold hopping and ROCS.

ROCS Shape Tanimoto					
BM212→ / Data set ↓	**Conf. 1**	**Conf. 2**	**Conf. 3**	**Conf. 4**	**Conf. 5**
Compound **4**	0.73	0.71	0.71	0.72	0.71
Compound **8**	0.73	0.71	0.7	0.68	0.66
Compound **12**	0.65	0.65	0.63	0.66	0.66

Table 2: The ROCS TSSC of compounds **4**, **8** and **12** with respect to different conformations of BM212

2 Results and Discussion

2.1 Molecular Design and Shape based complementarity studies with BM212

The scaffold hopping approach[11] was used to identify heterocycles that could replace the original core (pyrrole ring). **Figure 3** illustrates the shape of BM212 along with the pharmacophoric features that are essential for its bioactivity, namely, 1) a central hydrophobic core, 2) hydrogen bond acceptor and 3) two adjacent aromatic rings.

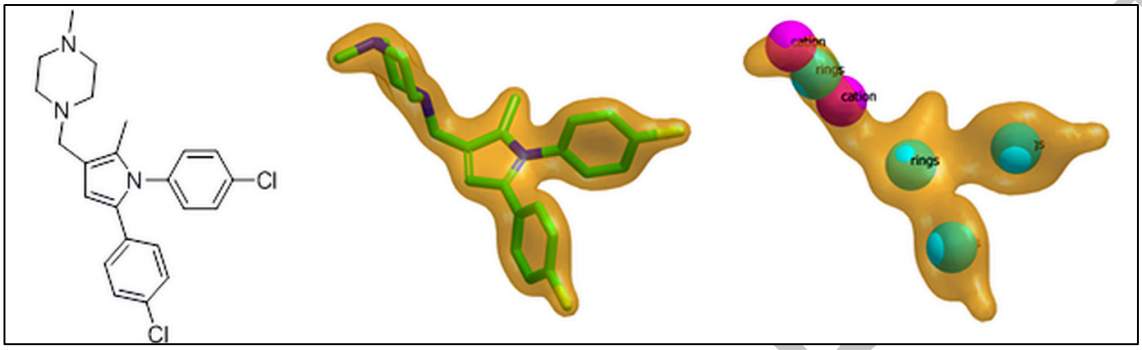

Figure 3 Representation of BM212 and pharmacophore features with its molecular shape.

The scaffold hopping approach identified imidazole, benzimidazole and imidazopyridine as three cores that could potentially replace the pyrrole ring. Derivatives of the identified cores were sought such that the 3D shape and volume of the new molecules were like the shape and volume of BM212. We surmised that by means of this strategy, the new derivatives would retain the potency inherent to BM212 (MIC 0.7-1.5 μg/ml). The Tanimoto shape similarity coefficient (TSSC) was used to quantify the shape similarity with BM212, and is expressed quantitatively in the range 0 to 1.0. A value of 1.0 indicates complete similarity, while 0 indicates no similarity (**Table 2**). A database curated from literature was virtually screened against the five lowest energy conformations of BM212. The 2,3-disubstitued benzimidazoles (e.g. compound **4)** with TSSC between 0.70 to 0.73 is closest in shape to BM212; next is the 1,2,4-trisubstituted imidazoles (e.g compound **8)** with TSSC 0.66 to 0.73, followed by the 2,3-disubstituted imidazopyridines (e.g. compound **12)** with TSSC 0.63 to 0.66. In case of 2,3-disubstituted benzimidazoles (**Figure 4a**), the two phenyl rings of benzimidazole superimpose well onto the two phenyl rings of BM212 and the benzimidazole core overlays the pyrrole ring. A similar arrangement is seen for the 1,2,4-trisubstituted imidazole (**Figure 4b**), the phenyl rings at the 1- and 2-positions overlap in a fashion similar to 2,3-disubstituted benzimidazole; the phenyl ring at the 4-position points towards the piperazine attached at the 3-position of BM212. With the 2,3-disubstituted imidazopyridines, the 2-phenyl ring overlaps with the 2-phenyl ring of BM212 (**Figure 4c**), however the 3-substituent (in this case the morpholine ring) as opposed to our expectations did not match

the piperazine moiety of BM212 but instead lies over the 3-phenyl ring of BM212.

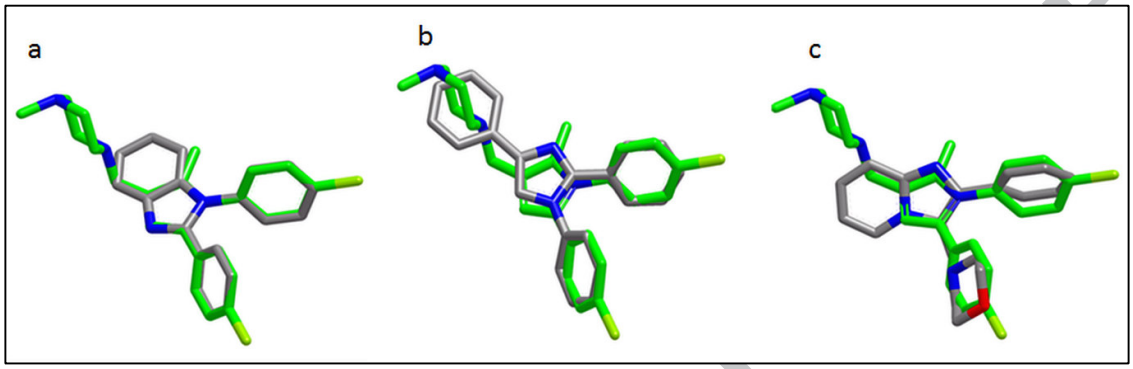

Figure 4: Molecular superimposition of **a**- compound **4**, **b**- compound **8**, and **c**- compound **12** on BM212. Compounds **4**, **8** and **12** are represented in grey color while the BM212 is shown in green color.

2.2 Chemistry

Synthesis of 2,3-disubstituted benzimidazoles[12] **(4a-4k)**, 1,2,4-trisubstituted imidazoles[13] **(8a-8b)** and 2,3-disubstituted imidazopyridines[14,15] **(12a-12g)** are described in Schemes **1–3**. Scheme **1** shows a one pot synthetic route for 2,3-disubstituted benzimidazoles using o-fluoro-nitrobenzene **(1)**, a substituted aniline **(2)** and a substituted benzaldehyde **(3)**. Substituted 1,2,4-trisubstituted imidazoles were synthesized as shown in Scheme **2**, in which a substituted aniline **(6)**, a substituted benzaldehyde **(7)**, ammonium acetate and phenacylbromide **(5)** are heated at 130^{o}C without any solvent. 2,3-Disubstituted imidazopyridines were synthesized in two steps (Scheme **3**) as follows: in the first step, 2-phenyimidazopyridines **(11)** were synthesized by cyclization of a substituted 2-aminopyridine **(9)** and a substituted phenacylbromide **(10)**. Then, in the second step, morpholine or piperidine was attached via a methyl linker at the 3-position of the imidazopyridine by the Mannich reaction.

2.2.1 Scheme 1 Synthesis of 2,3-disubstituted benzimidazoles

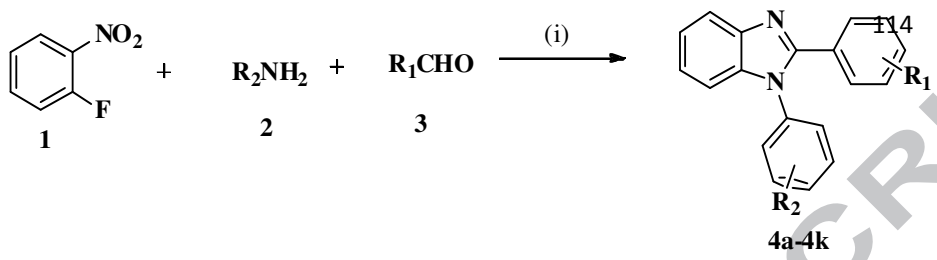

(i) DMSO, sodium dithionite, 130°C.

2.2.2 Scheme 2 Synthesis of 1,2,4-trisubstituted imidazoles

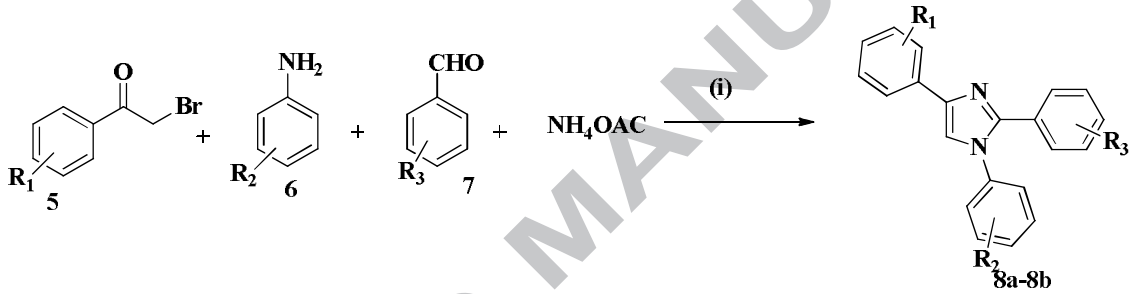

(i) 130°C for 2 Hrs.

2.2.3 Scheme 3 Synthesis of 2,3-disubstituted imidazo[1,2-a]pyridine

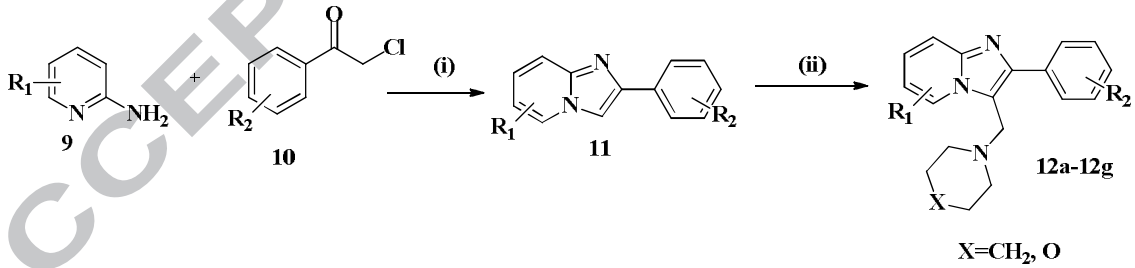

(i) ethanol, reflux (ii) acetic acid, morpholine/piperidine, ~ 36% formalin solution, room temperature.

2.3 Biological evaluation

2.3.1 Antitubercular activity

The antitubercular activity was measured on *Mycobacterium tuberculosis* H37Rv strain by the microplate alamar blue assay (MABA) as per published protocols[16]. The initial

concentration of the compounds was fixed at 50 µg/ml (**Table 3**). Alamar blue is a general indicator used to check cellular growth and/or viability; basically, the blue non-fluorescent oxidized form of the dye resazurin in the reducing environment of living cells turns into resorufin which is fluorescent pink. An inhibitor of mycobacterial growth will prevent this color change. Rifampicin and isoniazid were used as standards. Compounds that showed 95% inhibition at 50 µg/ml were further evaluated at lower concentrations to finally determine the minimum inhibitory concentration (MIC) for 95% inhibition. The results show that six compounds are active at less than 20 µg/ml against *Mycobacterium tuberculosis* H37Rv. The most potent compound **4a** has MIC of 2.3µg/ml.

The 2,3-disubstituted benzimidazoles were found to be the most promising among the three classes of molecules with MICs of 2.3 and 8.0 µg/ml for **4a** and **4b** respectively. On closer inspection, we find that for optimal antitubercular activity, the 4-methoxy group as R_1 and the 4-chloro substitution as R_2 on the benzimidazole ring are critical. A shift in the position of the R_1 methoxy group from the *para* to the *meta* position lowers the activity (**4h**, MIC >50 µg/ml), as also the addition of a methoxy group at the *ortho* position e.g. **4c and 4k** with MICs of 48.3 µg/ml and 20.3 µg/ml respectively. We also notice that the antitubercular activity is very sensitive to the R_2 substituent; moving the chloro substituent from the *para* to the *meta* position leads to complete abolishment of activity, e.g. **4f** (MIC >50 µg/ml, 0% inhibition). Further, we observe that replacing the chloro substituent with other halogens like bromine (**4d**, MIC >50 µg/ml, 92% inhibition) or fluorine (**4g**, MIC >50 µg/ml, 6% inhibition) leads to decrease in the activity. Replacement of the chloro substituent, with 2,5-dimethyl (**4e**, MIC >50 µg/ml, 80% inhibition) or 4-isopropyl (**4i**, MIC >50 µg/ml, 68% inhibition) or 3-methoxy (**4i**, MIC > 50 µg/ml, 14% inhibition) is detrimental to the activity. A drastic drop in the antitubercular activity, indicates that the chloro substituent at R_2 is essential.

In the 1,2,4-trisubstituted imidazole series, two molecules (**8a** and **8b**), have MICs of 20.3 µg/ml (**8a**) and 17.8 µg/ml (**8b**). Both molecules contain at the 4^{th} position of the 2-substituted phenyl ring, a hydrogen bond donor/acceptor group which is in line with the pharmacophore requirement for good antitubercular activity.

In the 2,3-disubstituted imidazopyridine class, five of the seven compounds have MICs below 50 µg/ml; these are **12c** with MIC of 17.0 µg/ml, **12a** with MIC of 22.2 µg/ml, **12b** MIC 23.9 µg/ml, **12f** MIC 33.7 µg/ml and **12d** MIC 40 µg/ml. This highlights the potential of 2,3-disubstituted imidazopyridines to be developed as new antitubercular agents. Interestingly, a minor change in the position of the methyl group from the 6th to the 7th position of the imidazopyridine ring, removal/addition of the 4-fluoro group on the 2-phenyl ring and replacement of the morpholine moiety with piperidine, show dramatic effects on the antitubercular activity. The methyl group on the 6th position of the imidazopyridine ring and the 4-fluoro on the 2-substituted phenyl ring impart the highest antitubercular activity as seen in compound **12c** with MIC of 17.0 µg/ml. A change in the position of the methyl group from the 6th to the 7th position as in compound **12b** results in a slight drop in the activity with MIC of 23.9 µg/ml. Removal of the methyl group but retaining the 4-fluoro group, as in **12c** and **12a,** preserve the antitubercular activity; however, removal of the 4-fluoro group while retaining the 7-methyl group as in **12d,** weakens the activity (MIC 40 µg/ml). Hence, we reckon that both the methyl and fluoro groups on the imidazopyridine ring are imperative for antitubercular activity, as is evinced by the MIC values of molecules **12g**, **12e** and **12f**

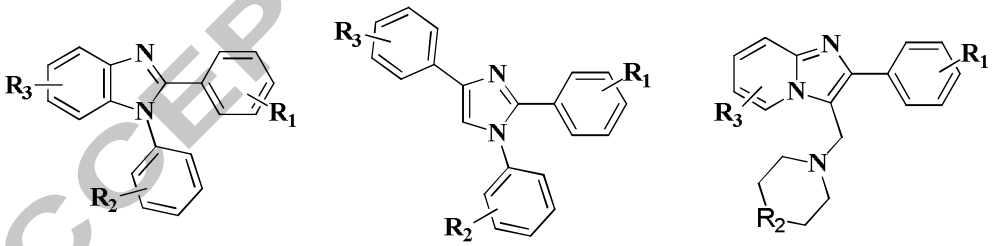

4a-4b **8a-8b** **12a-12g**

Comp.	R_1	R_2	R_3	*M. tuberculosis* H37Rv MIC (µg/mL)
4a	4-OCH_3	4-Cl	H	2.3

4b	4-OCH_3, 3-OH	H	H	8.0
8a	4-OCH_3	H	H	20.3
8b	4-OH	H	H	17.8
12a	O	4-F	H	22.2
12b	O	4-F	7-CH_3	23.9
12c	O	4-F	6-CH_3	17.0
12d	O	H	7-CH_3	40.0
12e	CH_2	H	H	>50
12f	CH_2	H	7-CH_3	33.7
12g	O	H	H	>50
Isoniazid				0.11
Rifampicin				0.03
A larger library of 2,3-disubstituted benzimidazoles				
4c	2,4-di(OCH_3)	4-Cl		48.3
4d	4-OCH_3	4-Br		> 50 (92)
4e	4-OCH_3	2,5-di(CH_3)		> 50 (80)
4f	4-OCH_3	3-Cl		> 50 (0)
4g	4-OCH_3	4-F		> 50 (6)
4h	3-OCH_3	4-Cl		> 50 (67)

4i	4-OCH_3	4-$CH(CH_3)_2$	> 50 (68)
4j	4-OCH_3	3-OCH_3	> 50 (14)
4k	3,4-di(OCH_3)	4-Cl	20.3
Isoniazid			0.06
Rifampicin			0.50

Table 3 Structures and *in vitro* antitubercular activity against *M. tuberculosis* H37Rv.

2.3.2 Assessment of selectivity – antitubercular vs antimicrobial/antifungal activity

In order to access how selective are the compounds against tuberculosis, we decided to evaluate the compounds for their activity on gram negative bacteria *Escherichia coli*, *Klebsiella pneumoniae, Acinetobacter baumannii, Pseudomonas aeruginosa,* the gram positive bacteria *Staphylococcus aureus*, and the fungi *Candida albicans* and *Cryptococcus neoformans* (**Table 4**). Expect for compounds **4d**, **4h** and **4j** with 50% inhibition of *Actinobacter baumanni* at the relatively high dose of 32 µg/ml, others show poor antibacterial and antifungal activity and is in sharp contrast to their antitubercular activity. This result highlights the selectivity of these molecules against *Mycobacterium tuberculosis* over gram positive bacteria, gram negative bacteria and fungi. The reason for this selectivity is unknown at present.

Test comp.	Percent inhibition at 32 µg/ml													
	Staphylococcus aureus (G +ve)		*Escherichia coli* (G -ve)		*Klebsiella. pneumoniae* (G -ve)		*Acinetobacter baumannii* (G -ve)		*Pseudomonas aeruginosa* (G -ve)		*Candida albicans* (Fungi)		*Cryptococcus neoformans var. grubii* (Fungi)	
	Strain ATCC43300		Strain ATCC 25922		Strain ATCC 700603		Strain ATCC 19606		Strain ATCC 27853		Strain ATCC 90028		Strain ATCC 208821	
	Inh. 1	Inh.2	Inh. 1	Inh.2	Inh. 1	Inh.2	Inh. 1	Inh.2	Inh. 1	Inh.2	Inh. 1	Inh.2	Inh. 1	Inh.2
4a	-19.12	4.59	-6.11	-6.64	2.12	-20.26	-3.17	32.03	9.75	1.34	12.9	12.19	-12.27	-2.00
4b	7.70	15.48	-8.29	-6.80	5.26	-1.42	-9.27	-0.58	7.73	1.32	11.26	6.64	-6.62	-9.81
4c	10.95	14.19	-5.75	-7.22	9.39	3.25	-6.12	1.56	8.86	-34.01	3.53	2.68	-10.75	-15.36
4d	12.30	15.00	-5.33	-12.42	7.06	-12.80	1.56	**58.14**	3.52	-28.18	11.65	9.75	14.66	-9.29
4e	10.01	9.57	-8.47	-11.99	14.01	-17.93	3.50	38.80	5.72	19.67	4.32	1.69	-7.27	-8.42
4f	15.99	14.12	-3.59	-6.55	12.72	-3.40	-7.86	-12.48	7.07	24.46	7.76	4.66	-3.58	-12.59
4g	12.65	11.62	-4.10	-7.46	6.63	-5.95	-9.90	-8.46	5.18	12.82	1.62	1.69	-12.49	-13.28
4h	-13.23	7.95	-8.63	-15.77	-3.23	-3.27	**50.78**	**49.38**	2.25	13.04	28.10	4.73	19.65	6.16
4i	6.25	12.36	-5.93	-11.64	2.46	-7.58	23.76	36.14	6.29	15.74	14.16	13.05	7.06	11.02
4j	7.42	20.44	-3.74	-5.29	8.57	-1.06	19.72	**59.86**	11.23	9.80	5.26	8.76	-8.36	-3.73
4k	1.03	9.81	-10.30	-15.61	-3.37	7.53	39.94	42.64	-3.23	19.16	7.63	8.23	4.02	0.95
8a	3.07	13.34	-5.08	-6.92	-0.26	-3.93	23.06	34.76	2.98	16.56	17.53	26.40	-18.35	-19.70
12a	22.29	30.28	-2.98	-13.56	13.72	-2.71	-5.84	8.91	11.03	14.35	0.63	5.39	1.63	-11.02

12b	20.12	21.75	-4.19	-12.41	14.39	-5.28	0.94	-16.15	9.71	26.98	2.74	7.44	-1.19	-2.86
12c	25.15	26.23	-2.48	-6.51	14.46	-6.29	-1.99	1.09	9.45	-2.06	6.17	3.40	1.85	-0.09
12d	15.85	23.49	-7.53	-12.61	7.77	-1.06	-9.54	-5.58	10.63	15.15	1.68	0.89	-11.62	-9.98
12e	14.77	19.41	-2.22	-12.91	11.72	-5.80	1.56	10.45	11.45	17.70	3.93	2.41	9.01	-4.43
12g	28.57	26.09	-2.72	-11.19	13.77	2.52	-2.71	6.13	9.04	16.50	0.30	6.38	2.71	3.04

189

190 **Table 4.** Antimicrobial and antifungal activity on selective strains

2.3.3 Cytotoxicity and Metabolic stability studies

A selected set of compounds were investigated for their cytotoxicity potential on normal kidney monkey cell lines[17] and HepG2 cell lines (**Table 5**). In this study, the concentration of a compound to inhibit 50% growth of the cells (GI_{50}), as well as the concentration to kill 50% of cells (LC_{50}) and finally the concentration to inhibit total growth of cells (TGI) were measured. Compounds **4a, 4b, 4c, 4d** and **4k** of the 2,3-disubstituted benzimidazole series were found to exhibit low cytotoxicity at concentrations below 10 μM against normal kidney monkey cell lines. The IC_{50} against HepG2 cell lines for compounds **4a, 4d** and **4k** were found to be 203.10 μM, 112.63 μM and 49.90 μM respectively. In the *in-vitro* metabolic stability studies compounds **4a, 4d** and **4k** were found to be metabolic stable in rat liver microsomes. There was no meaningful change found in the peak area ratio of compound to internal standard for compound **4a**, whereas **4d** and **4k** showed about 2% and 5% decrease respectively after 60 min of incubation. Overall it appears that the three compounds are stable to oxidative metabolism mediated by CYP450s and FMO. The positive control p-nitrophenol showed significant conversion to p-nitrocatechol (about 17%) in 60 minutes.

Comp.	*M. tuberculosis* H37Rv MIC (μg/mL)	Cytotoxicity studies				Metabolic stability studies
		Normal monkey kidney cell line VERO			HepG2 Cell line	% Turnover by rat liver microsomes in 60 min.
		GI_{50} (μM)	LC_{50} (μM)	TGI (μM)	IC_{50} (μM)	
4a	2.3	29	8.4×10^{5}	5×10^{3}	203.10	0
4b	8.0	4.5×10^{3}	-	-	-	-
4d	> 50 (92)	5.0	1×10^{3}	70	112.63	2
4k	20.3	8.2	5×10^{3}	200	49.90	5
ADR	-	0.02	0.2×10^{3}	2	-	-

Table 5 In vitro toxicity measured on normal monkey kidney cells and HEPG2 cell lines. GI_{50} = concentration of drug causing 50% inhibition of cell growth; LC_{50} = concentration of

drug causing 50% cell kill; TGI = concentration of drug causing total inhibition of cell growth; ADR = adriamycin, positive control.

3 Materials and Methods

All solvents and reagents used for the synthesis were of general reagent grade. All reactions were monitored by thin layer chromatography with Merck pre-coated silica plates (GF254). Column chromatography was used to purify the final products. Melting points were recorded using a Büchi capillary melting point apparatus and are uncorrected. Infrared spectra were recorded (KBr disc method) on a Jasco FT-IR 5300 spectrophotometer. NMR spectra were recorded on a Bruker Avance-II model with ^{1}H frequency of 400 MHz and ^{13}C resonance frequency of 100 MHz. Chemical shifts are reported in parts per million (ppm) downfield from tetramethylsilane (TMS) used as the internal standard. Mass spectra were recorded on an Agilent Technologies 1260 Infinity LC equipped with an Agilent Technologies 6120 Quadrupole mass spectrometer. Purity was evaluated by reversed-phase HPLC (RP-HPLC) on an Agilent Poroshell 120 EC-C18, 4.6 x 50 mm, 2.7 µm column with a flow rate of 1.5 mL/min. Compounds were eluted with gradient mixtures of A) 0.1% formic acid in water and B) Methanol. Compound purity was confirmed by elution with linear gradients of 95% A and 5% B for the initial 3.5 min, which was switched to 100% B for the 3.5 min to 7.5 min interval and finally to 95% A and 5% B for the last 7.5 to 10 min period. HPLC data are reported with percentage purity in parentheses following the retention time.

3.1 Computational details

Shape based similarity studies were carried out with the ROCS module in the Open Eye Scientific Software running on the Windows platform. ROCS can rapidly compare and rank molecules based on the three-dimensional shape similarity. To begin, various conformations of the reference molecule BM212 were generated using the confgen module in Schrödinger suite 2014, employing the OPLS 2005 forcefield to define the atom types, bond length, bond angles, torsions, improper and the intra-molecular non-bonded terms. The various conformations of BM212 were used to screen molecules by shape as the yard stick. Those closely related in shape and volume to BM212 were selected for structural optimization. Shape based screening was carried out on a database curated from the literature that comprised of different five membered, six membered and fused heterocyclic molecules. Of the various conformations generated for BM212, the five lowest energy structures were used as the query for shape-based screening. The TSSC was used to rank molecules which were then selected based on their Tanimoto score, synthetic feasibility and drug like properties. The last attribute i.e. drug likeness was assessed with the QikProp module in the Schrödinger

suite (Schrödinger LLC, New York, 2014).

3.2 Biological evaluation

3.2.1 Microplate Alamar Blue Assay and cytotoxicity studies -

All compounds were evaluated for their anti-TB activity against *Mycobacterium tuberculosis* $H_{37}Rv$ by the Microplate Alamar Blue assay (MABA) according to the well-established protocol, while cytotoxicity studies against Normal monkey kidney cells were carried out as per the protocol published by Kanyawim Kirtikara et. Al[17].

HepG2 Cytotoxicity Assay

Cell seeding was done by taking 100-200 µl of desired cell suspension (human Hepatocarcinoma Cell Line HepG2) in a 96-well plate at required cell density (25,000-50,000 cells per well), without the test agent. Cells were then allowed to adhere to the culture plate for about 24 hours. The plate was then incubated at 37°C in a 5% CO_2 atmosphere for 24 hours. After 24 hours the growth medium was removed and freshly prepared compound solutions were serially diluted (300µM, 100µM, 50µM, 10µM, 1µM 0.1µM). 100µl of each dilution in a 96 –well plate, in triplicates, were seed. After the incubation period of 24 hours, the plates were removed from the incubator and MTT reagent added to a final concentration of 10% of the total volume. This volume was the same volume that was used while determining the optimum cell density. The plate was wrapped in an aluminum foil to avoid exposure to light and put back into the incubator for 2 to 4 hours. The culture medium was then aspirated without disturbing the monolayer. Solubilization solution was then added (100% DMSO) in an amount equal to the culture volume and the solution stirred gently in a gyratory shaker to enhance the dissolution. The absorbance was read on a Spectostar Nano ELISA plate reader at 570 nm and IC_{50} values were calculated.

3.2.2 Antimicrobial and antifungal assay

Primary antimicrobial screening by whole cell growth inhibition was done in duplicate (n = 2) at a single concentration of 32 µg/mL. The study was carried out against five bacteria, namely, *Escherichia coli* (ATCC 25922), *Klebsiella pneumonia* (ATCC 700603), *Acinetobacter baumannii* (ATCC 19606), *Pseudomonas aeruginosa* (ATCC 27853) and *Staphylococcus aureus* (ATCC 43300), and two fungi: *Candida albicans* (ATCC 90028) and *Cryptococcus neoformans* (ATCC 208821). Samples were made up to 10 mg/mL in DMSO or water and stored frozen at -20°C. An aliquot of each sample was diluted to 320 µg/mL in water, and plated in 384-well polypropylene plates (PP). Five µL was plated in duplicate

(n=2) into a 384-well non-binding surface plate (NBS) for each strain or cell type assayed against. Once cells were added, the final compound concentration was 32 μg/mL and DMSO concentration was 0.3%. All bacteria were cultured in cation-adjusted Mueller Hinton broth (CAMHB) at 37°C overnight. A sample of each culture was then diluted 40-fold in fresh broth and incubated at 37°C for 1.5-3 h. The resultant mid-log phase cultures were diluted (CFU/mL measured by OD600), then 45 μL was added to each well of the compound containing plates, giving a cell density of 5×105 CFU/mL and the nominated final compound concentration. All plates were covered and incubated at 37°C for 18 h without shaking. Inhibition of bacterial growth was determined by measuring absorbance at 600 nm (OD600), using a Tecan M1000 Pro monochromator plate reader. The percent growth inhibition was calculated for each well, using the negative (media only) and positive controls (bacteria without inhibitors) on the same plate as references. The significance of the inhibition values was determined by Z-scores, calculated using the average and standard deviation of the sample wells (no controls) on the same plate. Samples with inhibition value above 50% and Z-Score above 2.5 for either replicate (n=2 on different plates) were classified as actives. For antifungal studies, fungal strains were cultured for 3 days on Yeast Extract-Peptone Dextrose (YPD) agar at 30°C. A yeast suspension of 1 x 10^6 to 5 x 10^6 cells/mL (as determined by OD530) was prepared from five colonies. These stock suspensions were diluted with Yeast Nitrogen Base (YNB) broth to a final concentration of 2.5 ×10 CFU/mL. Then, 45 μL of the fungi suspension was added to each well of the compound-containing plates, giving a final concentration of 32 μg/mL for the tested samples. Plates were covered and incubated at 35°C for 24 h without shaking. Inhibition of the growth of *C. albicans* was determined by measuring absorbance at 530 nm (OD530), while the inhibition of the growth of *C. neoformans* was determined by measuring the difference in absorbance between 600 and 570 nm (OD600-570), after the addition of resazurin (0.001% final concentration) and incubation at 35°C for additional 2 h. The absorbance was measured using a Biotek Synergy HTX plate reader. The percent growth inhibition was calculated for each well, using the negative (media only) and positive controls (fungi without inhibitors) on the same plate. The significance of the inhibition values was determined by Z-scores, calculated using the average and standard deviation of the sample wells (no controls) on the same plate. Samples with inhibition value above 50% and Z-Score above 2.5 for either replicate (n=2 on different plates) were classified as actives. Colistin and vancomycin were used as positive bacterial inhibitor standards for Gram negative and Gram-positive bacteria, respectively. Fluconazole was used as the positive fungal inhibitor standard for *C. albicans* and *C. neoformans.* The antibiotics

were provided in 4 concentrations, with 2 above and 2 below its MIC value, and plated into the first 8 wells of column 23 of the 384-well NBS plates. The quality control (QC) of the assays was determined by the antimicrobial controls and the Z'-factor (using positive and negative controls). Each plate was deemed to fulfill the quality criteria (pass QC), if the Z'-factor was above 0.4, and the antimicrobial standards showed full range of activity, with full growth inhibition at their highest concentration, and no growth inhibition at their lowest concentration. All antibiotic controls displayed inhibitory values within the expected range.

3.3 Synthesis

3.3.1 1-(4-Chlorophenyl)-2-(4-methoxyphenyl)-1H-benzo[d]imidazole (4a): In a round bottom flask 1 mmol. of 1-fluoro-2-nitrobenzene (**1**) and 1 mmol. of p-chloroaniline (**2**) in 2 ml of DMSO were heated for 2 h at 130°C. The completion of this step was verified by TLC. Then 1.5 mmol. of sodium dithionite and 1.2 mmol. of p-anisaldehyde (**3**) were added and heating was continued for 1 h. After completion of the reaction (monitored by TLC), water (10 mL) was added to the mixture and the solution was extracted with EtOAc (3 ×15 ml). The combined organic layer was washed with brine (5 ml) and dried over anhydrous Na_2SO_4. The residue obtained after evaporation of the organic solvent was purified by column chromatography with petroleum ether and ethyl acetate (7:3) as the mobile phase; this yielded the titled compound as light brown solid. (101.5 mg, 72%); m.p. 174-176ºC; ^{1}H-NMR (400 MHz, $CDCl_3$): δ = 3.82 (s, 3H), 6.83-6.87 (m, 2H), 7.19-7.28 (m, 4H), 7.31-7.35 (m, 1H), 7.46-7.51 (m, 4H), 7.84-7.86 ppm (d, J = 7.9 Hz, 1H); ^{13}C-NMR (100 MHz, $CDCl_3$): δ = 160.68, 152.32, 143.01, 136.94, 135.72, 134.35, 130.93, 130.15, 128.72, 123.23, 123.11, 121.96, 119.93, 113.93, 110.04, 55.30 ppm; IR (KBr): ν = 2924, 1269, 1300, 754 cm^{-1}; MS (EI, 70eV) m/z (%): 335.0 (100%), 337.0 (35%) [M + H]$^+$; HPLC t_R = 4.03 mins (98.06%).

3.3.2 1-Phenyl-2-(3-hydroxy-4-methoxyphenyl)-1H-benzo[d]imidazole (4b): Light brown solid (84.6 mg, 60%); m.p. 200-202ºC; ^{1}H-NMR (400 MHz, $CDCl_3$): δ = 3.81 (s, 3H), 5.79 (s, 1H), 6.69-6.71 (d, J = 8.4Hz, 1H), 7.02 (dd, J= 2.0, 8.4Hz, 1H), 7.07-7.08 (d, J = 2.1Hz, 1H), 7.13-7.46 (m, 8H), 7.78-7.80 ppm (d, J= 7.9Hz, 1H); ^{13}C-NMR (100 MHz, $CDCl_3$): δ = 152.04, 147.95, 146.94, 142.44, 136.94, 136.82, 129.75, 128.41, 127.35, 122.55, 122.31, 120.40, 118.73, 115.11, 112.72, 109.96, 55.09 ppm; IR (KBr): ν = 3392, 2936, 1305, 1256, 746, 1491 cm^{-1}; MS (EI, 70eV) m/z (%): 317.1 (100) [M + H]$^+$; HPLC t_R = 3.31 mins (94.35%).

3.3.3 1-(4-Chlorophenyl)-2-(2,4-dimethoxyphenyl)-1H-benzo[d]imidazole (4c): Light brown solid (91.7 mg, 65%); m.p. 96-98ºC; ^{1}H-NMR (400 MHz, $CDCl_3$): δ = 3.33 (s, 3H),

3.83 (s, 3H), 6.28-6.29 (d, J=2.2 Hz, 1H), 6.57 (dd, J = 2.2, 5.0 Hz, 1H), 7.17-7.19 (m, 2H), 7.26-7.31 (m, 1H), 7.31-7.32 (m, 2H), 7.34-7.38 (m, 2H), 7.57-7.59 (d, J = 8.4 Hz, 1H), 7.86 ppm (dd, J = 1.3, 8.9 Hz, 1H); ^{13}C-NMR (100 MHz, $CDCl_3$): δ = 162.65, 157.89, 151.31, 143.07, 136.04, 135.01, 133.17, 133.06, 129.25, 127.21, 123.16, 122.71, 119.87, 112.14, 109.96, 105.05, 98.37, 55.45, 54.71, 31.95, 29.72 ppm; IR (KBr): ν = 2925, 1494, 1211, 583, 1306 cm^{-1}; MS (EI, 70eV) m/z (%): 365.1 (100%), 367.1 (35%) $[M + H]^+$; HPLC t_R = 3.84 mins (99.25%).

3.3.4 1-(4-Bromophenyl)-2-(4-methoxyphenyl)-1H-benzo[d]imidazole (4d): Light brown solid (86.0 mg, 61%); m.p. 186-188ºC; ^{1}H-NMR (400 MHz, $CDCl_3$): δ = 3.82 (s, 3H), 6.84-6.87 (m, 2H), 7.19-7.27 (m, 4H), 7.31-7.35 (m, 1H), 7.47-7.51 (m, 2H), 7.62-7.65 (m, 2H), 7.84-7.86 ppm (d, J = 7.9 Hz, 1H); ^{13}C-NMR (100 MHz, $CDCl_3$): δ = 160.67, 152.27, 143.06, 136.86, 136.24, 133.14, 130.93, 129.01, 123.24, 123.12, 122.31, 121.95, 119.73, 113.94, 110.05, 55.32 ppm; IR (KBr): ν = 3048, 1481, 1253, 1107, 523 cm^{-1}; MS (EI, 70eV) m/z (%): 379.0 (100%), 381.0 (85%) $[M + H]^+$; HPLC t_R = 4.08 mins (99.26%).

3.3.5 1-(2,5-dimethylphenyl)-2-(4-methoxyphenyl)-1H-benzo[d]imidazole (4e): Light brown solid (80.4 mg, 57%); m.p. 166-168ºC; ^{1}H-NMR (400 MHz, $CDCl_3$): δ = 1.84 (s, 3H), 2.36 (s, 3H), 3.79 (s, 3H), 6.79-6.82 (m, 2H), 6.96-6.98 (d, J = 8.0 Hz, 1H), 7.18-7.20 (m, 1H), 7.22-7.22 (m, 1H), 7.24-7.28 (m, 2H), 7.30-7.32 (m, 1H), 7.54-7.58 (m, 2H), 7.84-7.86 ppm (d, J = 8.0 Hz, 1H); ^{13}C-NMR (100 MHz, $CDCl_3$): δ = 160.54, 152.20, 142.97, 137.37, 137.20, 135.96, 132.87, 131.43, 130.19, 130.07, 128.90, 122.83, 122.75, 122.66, 119.39, 113.83, 110.41, 55.25, 29.73, 20.91, 17.09 ppm; IR (KBr): ν = 2921, 1476, 1321, 1250 cm^{-1}; MS (EI, 70eV) m/z (%): 329.1(100) $[M + H]^+$; HPLC t_R= 3.98 mins (96.31%).

3.3.6 1-(3-Chlorophenyl)-2-(4-methoxyphenyl)-1H-benzo[d]imidazole (4f): White solid (56.4 mg, 40%); m.p. 202ºC; ^{1}H-NMR (400 MHz, $CDCl_3$): δ = 3.82 (s, 3H), 6.84-6.86 (d, 2H, J = 8.8 Hz), 7.17-7.47 (m, 6H), 7.47-7.47 (m, 1H), 7.49-7.51 (m, 2H), 7.84-7.86 ppm (d, J = 8.0 Hz, 1H); ^{13}C-NMR (100 MHz, $CDCl_3$): δ = 160.70, 152.26, 143.03, 130.37, 136.09, 135.41, 130.91, 128.81, 127.55, 125.90, 123.28, 123.17, 121.91, 119.73, 113.94, 110.08, 55.32 ppm; IR (KBr, cm^{-1}): ν = 3064, 1478, 1250, 1181, 613 cm^{-1}; MS (EI, 70eV) m/z (%): 335.0 (100%), 337.1 (35%) $[M + H]^+$; HPLC t_R = 4.04 mins (98.57%).

3.3.7 1-(4-Fluorophenyl)-2-(4-methoxyphenyl)-1H-benzo[d]imidazole (4g): Light brown solid (88.8 mg, 63%); m.p. 156-158ºC; ^{1}H-NMR (400 MHz,$CDCl_3$): δ = 3.81 (s, 3H), 6.82-6.85 (m, 2H), 7.17-7.25 (m, 2H), 7.26-7.34 (m, 5H), 7.47-7.51 (m, 2H), 7.84-7.86 ppm (d, J =

8.0 Hz, 1H); ^{13}C-NMR (100 MHz, $CDCl_3$): δ = 163.41, 160.93, 160.61, 152.43, 142.96, 137.23, 133.20, 133.16, 130.89, 129.30, 129.21, 123.15, 123.01, 122.08, 119.66, 117.07, 116.84, 113.87, 110.09, 55.30 ppm; IR (KBr): ν = 2962, 1475, 1266, 1248, 1054 cm^{-1}; MS (EI, 70eV) m/z (%): 319.1 (100) $[M + H]^+$; HPLC t_R= 3.76 mins (98.17%).

3.3.8 1-(4-Chlorophenyl)-2-(3-methoxyphenyl)-1H-benzo[d]imidazole (4h): Light brown solid (80.4 mg, 57%); m.p. 90-92ºC; ^{1}H-NMR (400 MHz, $CDCl_3$): δ = 3.74 (s, 3H), 6.90-6.93 (m, 1H), 7.01-7.36 (m, 8H), 7.45-7.49 (m, 2H), 7.87-7.89 ppm (d, J = 8.0 Hz, 1H); ^{13}C-NMR (100 MHz, $CDCl_3$): δ = 159.48, 152.10, 142.93, 136.96, 135.57, 134.44, 130.83, 130.14, 129.47, 128.66, 123.66, 123.26, 121.08, 120.03, 116.21, 114.23, 110.23, 55.29 ppm; IR (KBr): ν = 3053, 1491, 1322, 1271, 746 cm^{-1}; MS (EI, 70eV) m/z (%): 335.1 (100%), 337.1 (35%) $[M + H]^+$; HPLC t_R= 4.11 mins (98.20%).

3.3.9 1-(4-Isopropylphenyl)-2-(4-methoxyphenyl)-1H-benzo[d]imidazole (4i): Off white solid (73.3 mg, 52%); m.p. 154-156ºC; ^{1}H-NMR (400 MHz, $CDCl_3$): δ = 1.31-1.32 (s, 6H), 2.99-3.02 (m, 1H), 3.80 (s, 3H), 6.81-6.84 (m, 2H), 7.21-7.26 (m, 4H), 7.29-7.32 (m, 1H), 7.33-7.35 (m, 2H), 7.51-7.53 (m, 2H), 7.84-7.86 ppm (d, J = 7.9 Hz, 1H); ^{13}C-NMR (100 MHz, $CDCl_3$): δ = 160.45, 152.44, 149.34, 142.98, 137.41, 134.71, 130.90, 127.83, 127.26, 122.87, 122.74, 122.50, 119.47, 113.71, 110.46, 55.27, 33.86, 23.96 ppm; IR (KBr): ν = 2939, 1503, 1378, 1281 cm^{-1}; MS (EI, 70eV) m/z (%): 343.1 (100) $[M + H]^+$; HPLC t_R = 4.16 mins (98.69%).

3.3.10 1-(3-Methoxyphenyl)-2-(4-methoxyphenyl)-1H-benzo[d]imidazole (4j): Off white solid (88.8 mg, 63%); m.p. 152-154ºC; ^{1}H-NMR (400 MHz, $CDCl_3$): δ = 3.78 (s, 3H), 3.81 (s, 3H), 6.82-7.02 (m, 5H), 7.23-7.26 (m, 2H), 7.29-7.34 (m, 1H), 7.38-7.42 (m, 1H), 7.54 (dd, J = 2.1, 6.8 Hz, 2H), 7.84-7.86 ppm (d, J = 8.0 Hz, 1H); ^{13}C-NMR (100 MHz, $CDCl_3$): δ = 160.61, 160.54, 152.32, 142.90, 138.24, 137.19, 130.83, 130.59, 123.0, 122.86, 122.35, 119.75, 119.53, 114.26, 113.77, 113.09, 110.38, 55.53, 55.28 ppm; IR (KBr): ν = 2959, 1492, 1477, 1251 cm^{-1}; MS (EI, 70eV) m/z (%): 331.1 (100) $[M + H]^+$; HPLC t_R = 3.76 mins (98.04%).

3.3.11 1-(4-Chlorophenyl)-2-(3,4-dimethoxyphenyl)-1H-benzo[d]imidazole (4k): Light brown solid (77.6 mg, 55%); m.p. 162-164ºC; ^{1}H-NMR (400 MHz, $CDCl_3$): δ = 3.88 (s, 3H), 3.97 (s, 3H), 6.85-6.87 (d, J = 8.4 Hz, 1H), 7.07 (dd, J = 2.0, 8.4 Hz, 1H), 7.28-7.37 (m, 2H), 7.36-7.45 (m, 4H), 7.57-7.61 (m, 2H), 7.95-7.97 ppm (d, J = 7.9 Hz, 1H); ^{13}C-NMR (100 MHz, $CDCl_3$): δ = 152.54, 150.22, 148.74, 142.96, 137.01, 135.85, 134.41, 130.15, 128.02,

123.32, 123.15, 122.47, 122.07, 119.72, 112.33, 110.67, 110.05, 55.87, 55.80, 29.71 ppm; IR (KBr): ν = 2923, 1493, 1282, 1312, 765 cm^{-1}; MS (EI, eV) m/z (%): 365.1 (100%), 367.1 (38%) $[M + H]^+$; HPLC t_R = 3.93 mins (97.67%).

3.3.12 2-(4-Methoxyphenyl)-1,4-diphenyl-1H-imidazole (8a): A round bottom flask charged with1 mmol of phenacyl bromide (5), 1 mmol of aniline (6), 1 mmol of p-anisaldehyde (7) and 1.5 mmol of ammonium acetate were heated at 130°C for 2 h. After completion of the reaction (monitored by TLC), the reaction mixture was cooled to room temperature. The compounds were purified by column chromatography using petroleum ether and ethyl acetate (7:3) as the mobile phase; this yielded the titled compound as light brown solid (143.3 mg, 72%); m.p.196-198ºC; ^{1}H-NMR (400 MHz, $CDCl_3$): δ = 3.78 (s, 3H), 6.79 (dd, J = 1.8, 7.0 Hz, 2H), 7.24-7.28 (m, 3H), 7.37-7.43 (m, 8H), 7.87-7.89 ppm (m, 2H); ^{13}C-NMR (100 MHz, $CDCl_3$): δ = 49.99, 108.42, 112.89, 117.67, 119.78, 120.64, 121.68, 122.84, 123.35, 124.23, 124.96, 128.70, 133.39, 136.23, 141.75, 154.52 ppm; IR (KBr): ν = 2933, 1528, 1292, 1274 cm^{-1}; MS (EI, 70ev) m/z (%): 327.1 (100) $[M + H]^+$, HPLC t_R = 3.25 mins (88.85%).

3.3.13 2-(4-hydroxyphenyl)-1,4-diphenyl-1H-imidazole (8b): Light brown solid (131.3 mg, 66%); m.p. 233-234ºC; ^{1}H-NMR (400 MHz, $CDCl_3$): δ = 1.60 (s, 1H), 6.63 (dd, J = 2.0, 6.7 Hz, 2H), 7.21-7.43 (m, 11H), 7.85-7.87 ppm (m, 2H); ^{13}C-NMR (100 MHz, $CDCl_3$): δ = 157.64, 146.46, 140.15, 138.16, 133.91, 129.66, 129.21, 128.22, 127.81, 126.33, 125.57, 124.38, 120.90, 118.38, 114.87 ppm; IR (KBr): ν = 3422, 2924, 1493,1269, 1172 cm^{-1}; MS (EI, 70eV) m/z (%): 313.1 (100) $[M + H]^+$; HPLC t_R = 3.61 mins (99.64%).

3.3.14 2-(4-Fluorophenyl)-3-(morpholine-1-ylmethyl)imidazo[1,2-a]pyridine (12a):

Step 1 Synthesis of 4-Fluorophenyl-imidazo[1,2-a]pyridine (11)

In a round bottom flask, 2-aminopyridine (**9**) (1 mmol.) and 4-fluorophenacyl chloride (**10**) (1.5 mmol.) were added in 5 mL of ethanol and refluxed for 4-6 h. After cooling the reaction mixture, ethanol was removed *in vacuo* and the residue was treated with saturated $NaHCO_3$ solution (10 ml) and extracted with $CHCl_3$ (3×10 mL). The combined organic phases were dried over anhydrous Na_2SO_4. Removal of the solvent under reduced pressure gave the crude product which was purified by column chromatography using petroleum ether and ethyl acetate (7:3) as the mobile phase.

Step 2 Synthesis of 2-(4-fluorophenyl)-3-(morpholine-1-ylmethyl) imidazo[1,2-a] pyridine (12)

To a solution of 4-fluorophenyl-imidazo[1,2-a]pyridine (**11)** (1 mmol) in acetic acid (5 ml), morpholine (1.5 mmol) and ~ 36% formalin solution (1.5 mmol) were added slowly and stirred at 25-35°C until the reaction was complete. The reaction mixture was cooled to 0-10°C and the pH adjusted between 8-9 with 20% aqueous sodium hydroxide solution. The solid which precipitated out was filtered, washed with water, dried and purified by column chromatography using petroleum ether and ethyl acetate (7:3) as the mobile phase; this yielded the title compound as a white solid (173.8 mg, 82%); m.p. 176-178ºC; ^{1}H-NMR (400 MHz, $CDCl_3$) δ = 2.48 ppm (t, J = 4.4 Hz, 4H), 3.68 ppm (t, J = 4.5 Hz, 4H), 3.94 ppm (s, 2H), 6.86-6.87 (m, 1H), 7.13-7.18 (m, 2H), 7.22-7.26 (m, 1H), 7.62-7.64 (d, J = 9.0Hz, 1H), 7.76-7.80 (m, 2H), 8.41-8.43 ppm (d, J = 6.9Hz, 1H); ^{13}C-NMR (100 MHz, $CDCl_3$): δ = 163.02, 161.36, 145.04, 144.93, 144.38, 143.19, 130.56, 130.47, 130.44, 130.17, 130.09, 125.21, 125.09, 124.80, 124.47, 119.44, 117.21, 117.17, 115.79, 115.55, 115.47, 115.34, 115.26, 112.28, 112.05, 66.95, 53.75, 53.18, 52.02 ppm; IR (KBr): ν = 2965, 1501, 1374, 1358, 1112 cm^{-1}; MS (EI, 70eV) m/z (%): 312.1(100) $[M + H]^+$; HPLC t_R = 2.41 mins (99.68%).

3.3.15. 2-(4-Fluorophenyl)-7-methyl-3-(morpholine-1-ylmethyl)imidazo[1,2-a]pyridine (12b): White solid (180.8 mg, 80%); m.p. 196-198ºC; ^{1}H-NMR (400 MHz, $CDCl_3$) δ = 2.42 (s, 3H), 2.46 (t, J = 4.3 Hz, 4H), 3.67 (t, J = 4.5 Hz, 4H), 3.91 (s, 2H), 6.66-6.68 (m, 1H), 7.12-7.16 (m, 2H), 7.38 (s, 1H), 7.75-7.78 (m, 2H), 8.27-8.29 ppm (d, J = 7 Hz, 1H); ^{13}C-NMR (100 MHz, $CDCl_3$): δ = 163.73, 161.20, 145.51, 144.13, 135.66, 130.78, 130.74, 130.49, 130.41, 124.38, 115.64, 115.50, 115.28, 115.16, 114.63, 66.99, 53.17, 52.05, 21.37 ppm; IR (KBr): ν = 3070, 1503, 1375, 1358, 1114 cm^{-1}; MS (EI, 70eV) m/z (%): 326.1 (100) $[M + H]^+$; HPLC t_R = 2.57 mins (98.42%).

3.3.16. 2-(4-Fluorophenyl)-6-methyl-3-(morpholine-1-ylmethyl)imidazo[1,2-a]pyridine (12c): White solid (169.5 mg, 75%); m.p. 150-151ºC; ^{1}H-NMR (400 MHz, $CDCl_3$): δ = 2.38 (s, 3H), 2.48 (t, J = 4.5 Hz, 4H), 3.68 (t, J = 4.6 Hz, 4H), 3.90 (s, 2H), 7.08 (dd, J = 1.6, 9.1Hz, 1H), 7.12-7.16 (m, 2H), 7.52-7.54 (d, J = 9.1Hz, 1H), 7.77-7.80 (m, 2H), 8.15 ppm (s, 1H); ^{13}C-NMR (100 MHz, $CDCl_3$): δ = 163.74, 161.29, 144.31, 144.14, 130.79, 130.76, 130.50, 130.42, 127.84, 122.65, 121.61, 116.60, 115.50, 115.20, 66.99, 53.20, 51.99, 10.55 ppm; IR (KBr): ν = 2925, 1503, 1377, 1341, 1112 cm^{-1}; MS (EI, 70eV) m/z (%): 326.1(100) $[M + H]^+$; HPLC t_R = 2.59 mins (98.93%).

3.3.17 7-Methyl-2-phenyl-3-(morpholine-1-ylmethyl)imidazo[1,2-a]pyridine (12d): White solid (151.8 mg, 73%); m.p. 138-140ºC; ^{1}H-NMR (300 MHz, $CDCl_3$): δ = 2.36 (s, 3H), 2.46

(t, J = 9.0 Hz, 4H), 3.66 (t, J = 6.0 Hz, 4H), 3.95 (s, 2H), 6.71-6.75 (m, 1H), 7.37-7.50 (m, 4H), 7.75-7.80 (m, 2H), 8.32-8.36 ppm (d, J = 12.0 Hz, 1H); ^{13}C-NMR (100 MHz, $CDCl_3$): δ = 144.62, 143.38, 134.96, 134.52, 128.20, 128.16, 128.09, 128.05, 127.23, 127.15, 124.62, 115.38, 114.84, 114.77, 114.11, 66.22, 52.66, 51.09, 20.83 ppm; IR (KBr): ν = 2943, 1504, 1358 cm^{-1}; MS (EI, 70eV) m/z (%): 308.2(100) $[M + H]^+$; HPLC t_R = 2.50 mins (98.55%).

3.3.18 2-Phenyl-3-(piperidin-1-ylmethyl)imidazo[1,2-a]pyridine (12e): White solid (128 mg, 66%); m.p. 127-128ºC; ^{1}H-NMR (300 MHz, $CDCl_3$): δ = 1.43-1.61 (m, 10H), 3.92 (s, 2H), 6.79-6.82 (m, 1H), 7.18-7.23 (m, 1H), 7.34-7.38 (m, 1H), 7.44-7,47 (m, 2H), 7.62-7.64 (d, J = 9.0 Hz, 1H), 7.81-7.83 (m, 2H), 8.49-8.51 ppm (d, J = 8.1 Hz, 1H); ^{13}C-NMR (100 MHz, $CDCl_3$): δ = 144.11, 144.03, 143.76, 142.95, 134.50, 134.28, 128.29, 128.22, 128.15, 128.09, 127.37, 127.20, 125.47, 124.86, 124.63, 124.28, 120.32, 116.06, 116.52, 116.39, 111.78, 111.47, 53.58, 52.33, 51.60, 25.59, 23.91 ppm; IR (KBr): ν = 2915, 1504, 1358 cm^{-1}; MS (EI, 70eV) m/z (%): 292.2(100) $[M + H]^+$; HPLC t_R = 1.72 mins (98.42%).

3.3.19 7-methyl-2-phenyl-3-(piperidin-1-ylmethyl)imidazo[1,2-a]pyridine (12f): White solid (166.4 mg, 80%); m.p. 70-72ºC; ^{1}H-NMR (300 MHz, $CDCl_3$): δ = 1.41-1.52 (m, 6H), 1.80 (m, 4H), 2.40 (s, 3H), 3.87 (s, 2H), 6.63 (m, 1H), 7.43-7.5 (m, 4H), 7.80 (m, 2H), 8.36 ppm (m, 1H); ^{13}C-NMR (100 MHz, $CDCl_3$): δ = 145.40, 144.34, 135.30, 134.84, 128.86, 128.34, 127.44, 124.89, 116.51, 115.44, 114.29, 54.22, 52.20, 26.10, 24.44, 21.37 ppm; IR (KBr): ν = 2937, 1502, 1340, 1361 cm^{-1}; MS (EI, 70eV) m/z (%): 306.2 (100) $[M + H]^+$; HPLC t_R = 1.86 mins (99.42%).

3.3.20 2-Phenyl-3-(morpholine-1-ylmethyl)imidazo[1,2-a]pyridine (12g): White solid (163.0 mg, 84%); m.p.141-143ºC; ^{1}H-NMR (300 MHz, $CDCl_3$): δ = 2.49 (t, 4H, J = 4.4 Hz), 3.68 (t, J = 4.6 Hz, 4H), 3.99 (s, 2H), 6.82-6.86 (m, 1H), 7.21-7.26 (m, 1H), 7.36-7.40 (m, 1H), 7.45-7.49 (m, 2H), 7.63-7.66 (m, 1H), 7.79-7.81 (m, 2H), 8.44 ppm (dd, J = 1.0, 5.7Hz, 1H); ^{13}C-NMR (100 MHz, $CDCl_3$): δ = 145.31, 145.10, 134.43, 128.88, 128.57, 128.47, 128.41, 127.78, 125.32, 124.60, 117.25, 115.91, 111.90, 66.98, 53.20, 52.11 ppm; IR (KBr): ν = 2859, 1499, 1354, 1268 cm^{-1}; MS (EI, 70eV) m/z (%): 294.1(100) $[M + H]^+$; HPLC tR = 2.30 mins (95.32%).

4 Conclusions

In our efforts to identify novel antitubercular agents, we adopted BM212 as the lead molecule and identified imidazoles, benzimidazoles and imidazopyridines as being similar to BM212 based on shape/volume features. With the scaffold hopping approach we designed and

synthesized a small library of 20 molecules belonging to the three structurally diverse heterocycles, namely 2,3-disubstituted benzimidazole, 1,2,4-trisubstituted imidazole, and 2,3-disubstituted imidazopyridine. These molecules were screened against *Mycobacterium tuberculosis* and the 2,3-disubstituted benzimidazoles emerged as the most active antitubercular agents; the most potent molecule (**4a**) in this series has an MIC of 2.3 μg/ml. It is reassuring to note that molecule **4a** (MIC 2.3 μg/ml) identified in this work is as potent as the lead molecule BM212 (MIC 0.7 to 1.5 μg/ml), however it is superior to BM212 in that it shows no toxicity in VERO as well as HEPG2 cell lines and is also not metabolized by rat liver microsome. The antimicrobial and antifungal activity shows **4a** to be selective against *Mycobacterium tuberculosis*.

References

1. World Health Organization. "Global tuberculosis report 2016." (2016).
2. Deidda D, Lampis G, Fioravanti R, et al. Bactericidal activities of the pyrrole derivative BM212 against multidrug-resistant and intramacrophagic Mycobacterium tuberculosis strains. *Antimicrobial agents and chemotherapy.* 1998;42(11): 3035-3037.
3. Biava, Mariangela, et al. Antimycobacterial agents. Novel diarylpyrrole derivatives of BM212 endowed with high activity toward Mycobacterium tuberculosis and low cytotoxicity. *Journal of medicinal chemistry.* 2006; 49(16): 4946-4952.
4. Alfonso S. BM212-derived MmpL3 inhibitors enabling new possibilities for the treatment of TB and studies of mycobacterial iron assimilation as new potential target for drug discovery. PhD Thesis; 2013.
5. Biava M, Porretta GC, Poce G, et al. Developing Pyrrole-Derived Antimycobacterial Agents: a Rational Lead Optimization Approach. *ChemMedChem.* 2011;6(4): 593-599.
6. Poce G, Bates RH, Alfonso S, et al. Improved BM212 MmpL3 inhibitor analogue shows efficacy in acute murine model of tuberculosis infection. *PLoS One.* 2013;8(2): e56980.
7. Bhakta S, Scalacci N, Maitra A, et al. Design and Synthesis of 1-((1, 5-Bis (4-chlorophenyl)-2-methyl-1 H-pyrrol-3-yl) methyl)-4-methylpiperazine (BM212) and N-Adamantan-2-yl-N′-((E)-3, 7-dimethylocta-2, 6-dienyl) ethane-1, 2-diamine (SQ109) Pyrrole Hybrid Derivatives: Discovery of Potent Antitubercular Agents Effective against Multidrug-Resistant Mycobacteria. *Journal of medicinal chemistry.* 2016;59(6): 2780-2793.

8. Rush TS, Grant JA, Mosyak L, Nicholls A. A shape-based 3-D scaffold hopping method and its application to a bacterial protein-protein interaction. *Journal of medicinal chemistry.* 2005;48(5): 1489-1495.

9. Nicholls A, MacCuish NE, MacCuish JD. Variable selection and model validation of 2D and 3D molecular descriptors. *Journal of computer-aided molecular design.* 2004;18(7-9): 451-474.

10. Grant JA, Gallardo M, Pickup BT. A fast method of molecular shape comparison: A simple application of a Gaussian description of molecular shape. *Journal of computational chemistry.* 1996;17(14): 1653-1666.

11. Schneider G, Neidhart W, Giller T, Schmid G. "Scaffold-Hopping" by Topological Pharmacophore Search: A Contribution to Virtual Screening. *Angewandte Chemie International Edition.* 1999;38(19): 2894-2896.

12. Roy P, Pramanik A. One-pot sequential synthesis of 1, 2-disubstituted benzimidazoles under metal-free conditions. *Tetrahedron Letters.* 2013;54(38): 5243-5245.

13. Adib M, Ansari S, Feizi S, Damavandi JA, Mirzaei P. A one-pot, four-component synthesis of N-substituted 2, 4-diarylimidazoles. *Synlett.* 2009;2009(20): 3263-3266.

14. Fisher MH, Lusi A. Imidazo [1, 2-a] pyridine anthelmintic and antifungal agents. *Journal of medicinal chemistry.* 1972;15(9): 982-985.

15. Lombardino JG. Preparation and new reactions of imidazo [1, 2-a] pyridines. *The Journal of Organic Chemistry.* 1965;30(7): 2403-2407.

16. Franzblau SG, Witzig RS, McLaughlin JC, et al. Rapid, low-technology MIC determination with clinical Mycobacterium tuberculosis isolates by using the microplate Alamar Blue assay. *Journal of clinical microbiology.* 1998;36(2): 362-366.

17. Vichai V, Kirtikara K. Sulforhodamine B colorimetric assay for cytotoxicity screening. *Nature protocols.* 2006;1(3): 1112-1116.

Acknowledgements

The authors are thankful to the Council of Scientific and Industrial Research, New Delhi (File no. 02(0047)/12/EMR-II), Department of Biotechnology, New Delhi (File No. BT/PR11810/BRB/10/690/2009) and Department of Science and technology, New Delhi through their FIST program (SR/FST/LSI-163/2003) for providing computational and infrastructural facilities. Antimicrobial screening was performed by CO-ADD (The Community for Antimicrobial Drug Discovery) funded by the Wellcome Trust (UK) and The University of Queensland (Australia). In vitro SRB assay for cytotoxicity studies was done at

Anti-Cancer Drug screening facility (ACDSF) at ACTREC, Tata Memorial Centre, Navi Mumbai, India. The HEPG2 toxicity studies was carried out at Genelon Institute of Life Sciences Pvt. Ltd., Bengaluru, India.